

# The chemistry of deposits formed from acrylic acid plasmas

Morgan R. Alexander\* and Tran M. Duc

CENATS (University Claude Bernard Lyon-1) c/o BIOPHY Research S A, Village d'Entreprises de St Henri, 6 rue Anne Garcon, Marseille 13016, France

SIMS and XPS were used to characterise the chemistry of thin plasma polymerised acrylic acid films (ppAAc), and to determine how this was influenced by plasma power. Quartz microbalance weight measurements were used to monitor the effect of power on the deposition rate and identify the uptake of water vapour by the films upon exposure to the atmosphere. Functional group derivatisation and XPS were used to quantify the proportion of carboxylic acid and ester functionalities. Derivatisation revealed that the level of retention in the deposit could be controlled by the plasma deposition power ( $P$ ) up to a maximum of 66% at  $P = 2$  W. TOF SIMS analysis identified the presence of linear structures with up to five monomer units in the high retention deposit. The role of such structures in functional retention is discussed with reference to mass spectrometry data in the literature.

A polymeric film deposited on a substrate from a 'cold' radio frequency plasma sustained in the vapour of an organic compound is referred to as a plasma polymer. The fabrication and characterisation of a wide range of plasma polymers has been the subject of many publications.<sup>1,2</sup> Interest in such materials lies in their unique coating properties which include: good adherence, 'pin-hole' free and conformal coating of substrates. The attributes commonly cited for the application of plasma deposits are their diffusion, optical, hardness and abrasion properties.<sup>3</sup> However, recently there has been much interest in the chemistry of such novel coatings and how it may be used to modify the surface chemistry of conventional materials. Specifically, recent work has explored the retention of carboxylic acid, hydroxy, ester, sulfone and amine monomer functionalities, in the plasma polymer deposit.<sup>4-13</sup>

Chemical surface modification using plasma polymers has potential applications in adhesion promotion.<sup>4,5</sup> The effectiveness of plasma polymerised acrylic acid (ppAAc) in improving interfacial shear strength between carbon fibre and epoxy resin has recently been demonstrated.<sup>12,13</sup> Good interfacial bonding was obtained between epoxy resin and carbon fibre coated with a thin film of ppAAc. This was attributed to the formation of covalent bonds between the carboxy groups at the surface of the deposit and the epoxy functionalities in the resin, in addition to a strong plasma polymer-carbon fibre bond. Combined with inert-gas-plasma surface activation and cleaning a good bond may be achieved between plasma polymers and a wide range of materials.

Within this paper we present a quantitative description of the surface chemistry of acrylic acid plasma polymer determined using surface analytical techniques. Such techniques are appropriate for the characterisation of such materials present in small quantities as thin films. Previously, the surface chemistry of ppAAc has been characterised to a limited extent by XPS where the main aim of the work was adhesion promotion,<sup>4,5</sup> reduction of platelet adhesion<sup>7</sup> and determination of the plasma phase polymerisation mechanisms by plasma mass spectrometry.<sup>10</sup> In all these papers the description of the chemistry was limited by a lack of quantitative derivatisation to distinguish the acid functionalities from the esters. Herein, quantification of the surface functional composition, and how this is affected by plasma power ( $P$ ), is achieved by X-ray photoelectron spectroscopy (XPS) and trifluoroethanol (TFE) carboxy group derivatisation. Additionally, secondary ion mass spectrometry (SIMS) analysis of the films provides structural molecular information which we are able to relate to oligomeric species previously identified in the plasma by mass spectrometry.<sup>10</sup>

## Experimental

### Plasma deposition

The plasma deposition system consisted of the elements schematically illustrated in Fig. 1. This apparatus comprised a radio frequency power source (13.56 kHz) with manual power matching which was tuned to minimise the reflected power ( $<1$  W). This was capacitively coupled *via* two copper bands to a deposition chamber evacuated to a base pressure of approximately 1 Pa. The deposition chamber comprised a cylindrical borosilicate glass T-piece sealed with stainless steel end-plates using PTFE o-rings. Acrylic acid (Aldrich) monomer was degassed using a freeze-thaw cycle. The flow of acrylic acid vapour into the reaction vessel was regulated through the use of manually operated needle valves. The monomer flow rate was monitored before and after the deposition, and found to remain constant for a fixed leak-valve setting. All plasma polymer samples in this paper were produced at an acrylic acid flow rate of  $5 \text{ cm}^3_{\text{STP}} \text{ min}^{-1}$  (sccm). The pressure in the chamber before the plasma was initiated was kept constant (40 Pa) using a valve on the pumping line. A liquid nitrogen cold trap and an alumina trap were used to prevent fouling of the rotary pump with condensable plasma products and contamination of the reaction chamber by pump oil (Fomblin). Deposition weight measurements were made using an STM-100/MF vibrating quartz crystal microbalance (Sycon Instruments New York) which utilised a gold coated quartz crystal with an exposed area of diameter 9 mm. The mass of deposited film was determined by measurement of the resonance frequency of the exposed quartz crystal.

For analysis, the ppAAc was deposited on aluminium foil positioned downstream of the region where the plasma was formed. All samples were of thickness greater than that of the XPS and SIMS analysis depths, such that the substrate signal

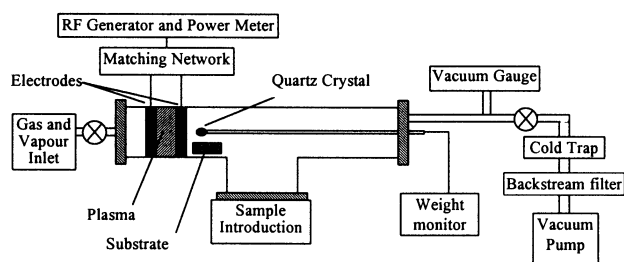


Fig. 1 Schematic of the plasma deposition apparatus

did not interfere with the deposit analysis. Samples were stored in aluminium foil envelopes at ambient conditions.

## XPS

XPS spectra were acquired on a Scienta ES200 spectrometer. A monochromated Al-K $\alpha$  X-ray beam ( $4 \times 0.2$  mm) of 500 W was used to generate the emission of photoelectrons from the surface of the sample, analysed at a take-off angle ( $\phi$ ) of  $90^\circ$ . Thus, the analysis depth ( $d$ ), from which 95% of the photoelectrons contributing to the spectra emanate, may be estimated to be 7 nm for C 1s and 8 nm for Al 2p photoelectrons ( $d = 3\lambda \sin \phi$  where  $\lambda = 2.40$  nm for C 1s and 2.75 nm for Al 2p electrons).<sup>14</sup>

Quantification of the spectra was undertaken, after correction of the spectral intensity for the spectrometer transmission function, using sensitivity factors calculated from Scofield cross-sections. Verification of the accuracy of these factors, and correction where necessary, was performed using standard compounds. We estimate that using this method an accuracy of  $\pm 10\%$  in the measurement of the elemental composition was achieved. The concentrations presented from XPS data are in atomic percent excluding hydrogen which the technique does not detect. The error bars on the elemental composition in Fig. 3, 5 and 6 were calculated from the analysis of nominally identical samples to provide a measure of the reproducibility of the data included in these figures.

Curve fitting of all C 1s peaks was carried out using the same initial conditions and inter-peak constraints for each spectra in order to reduce inter-sample scatter. The C 1s envelope from ppAAc was fitted with component peaks of equal full width half maximum (FWHM), except for the  $\beta$ -shifted carbon which was constrained to be 10% greater. This procedure was adopted on the basis of the C 1s curve fit of a poly(acrylic acid) (PAA).<sup>15</sup> The shape of the peaks was also kept equal, and varied between a Gaussian to Lorentzian (G/L) mix of 0.8–1. Again, the  $\beta$ -shifted carbon was an exception to this with a G/L mix of 10% less than the other components. The total intensity of the  $\beta$ -shift was constrained to equal to that of the well defined carboxylic acid component. The position of the C(–O) and C(–O)<sub>2</sub> components were fixed at 1.4–1.5 eV and 2.7–2.8 eV from the CH/C–C component respectively. Curve fitting of TFE-labelled ppAAc was conducted using the same procedure for peaks from the pre-labelled polymer. The position and FWHM of the two peaks from the TFE molecule (CF<sub>3</sub> and –O–CH<sub>2</sub>–CF<sub>3</sub>) were optimised while their intensities were constrained to be equal.

## Derivatisation

Trifluoroethanol (TFE) labelling of acid functionalities was carried out according to the protocol first detailed by Chilkoti *et al.*,<sup>16</sup> and later updated by Alexander *et al.*<sup>17</sup> This involved exposure of the samples to TFE vapour in the presence of a catalyst (pyridine) and a drying agent, di-*tert*-butylcarbodiimide (Di-tBuC) at room temperature. All reagents were purchased from Aldrich. The samples were placed on a microscope slide in a boiling tube which was sealed with a PTFE coated stopper. The reagents were introduced below the samples at 15 min intervals in quantities of 0.09, 0.04 and 0.03 ml respectively.

Instead of determining the time for full labelling of TFE with a standard compound, *e.g.* PAA, a fixation *vs.* time curve was constructed for ppAAc at the two extremes of the deposition conditions considered ( $P = 2$  and 20 W) to identify an appropriate exposure time for stoichiometric reaction. The rationale behind this approach is based on the potential non-stoichiometric reaction of TFE with certain chemistries as described in detail in ref. 17.

## SIMS

SIMS was carried out on a PHI 7200 instrument, using a 8 keV Cs primary ion beam and electron charge neutralisation. The cumulative primary ion dose for both positive and negative spectra was less than  $1 \times 10^{12}$  ions  $\text{cm}^{-2}$ .

## Results

### Deposit weight measurements

Using a vibrating quartz crystal microbalance it was possible to measure the weight of plasma polymer deposited on a quartz crystal during the plasma polymerisation process. The rate of deposition was found to remain constant with deposition time. The deposition rate is plotted as a function of deposit power ( $P$ ) in Fig. 2. It is apparent that increasing  $P$  to 4 W had the effect of raising the deposition rate to a maximum of  $2 \mu\text{g min}^{-1}$  [ $31 \text{ nm min}^{-1}$ , assuming a plasma polymer density ( $\rho$ ) =  $1 \text{ g cm}^{-3}$ ]. Increasing  $P$  further resulted in a gradual decrease in deposition rate.

Immediately after the RF power was turned off the weight of the deposit was observed to increase slightly (0.03–0.13  $\mu\text{g}$ ). This weight gain occurred within the first 15 s after the plasma power was turned off and was fully removed when the chamber was evacuated of monomer. This effect is attributed to adsorption/absorption of acrylic acid molecules by the deposit which desorb when the monomer flow is stopped and the chamber is evacuated to the base pressure. Leaving the deposit in the monomer flow for longer before evacuation brought no permanent increase in the deposit weight.

It was also possible to monitor weight changes that occur upon venting the chamber to atmospheric pressure after the monomer flow was stopped and the chamber evacuated. Venting of the deposition chamber to dry air resulted in the same increase in weight of 0.16  $\mu\text{g}$ ; both with a new sensor before deposition of a coating, and with a 26  $\mu\text{g}$  coating of  $P = 2$  W ppAAc deposit. This effect may therefore be attributed to the adsorption of oxygen and nitrogen molecules on the crystal/pp surface. Venting the deposition chamber to air, from the ambient atmosphere, provided a greater weight increase, of 1.36  $\mu\text{g}$ , which was fully reversible upon reevacuation of the chamber. This weight gain was assigned to the pick-up of atmospheric moisture by the polymer in addition to the adsorbed N<sub>2</sub> and O<sub>2</sub>. The magnitude of this water pick-up was determined to be linearly related to the total weight/thickness of the deposit and was thus assigned to water absorption within the polymer film. The absorption of water from the atmosphere to an equilibrium concentration (up to 7 wt% H<sub>2</sub>O has been observed) was found to be dependent upon  $P$  and the relative humidity of the air. This phenomenon, and its interrelationship with deposit chemistry, will be fully

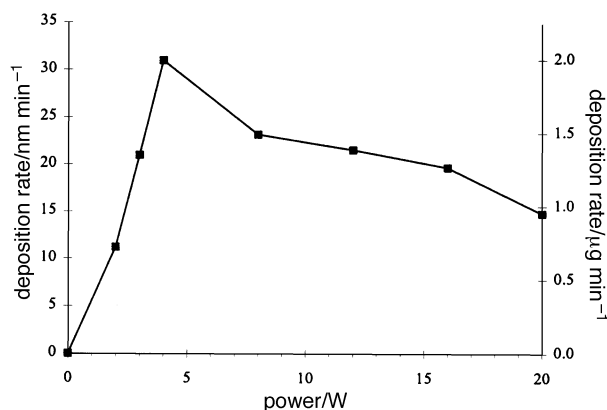
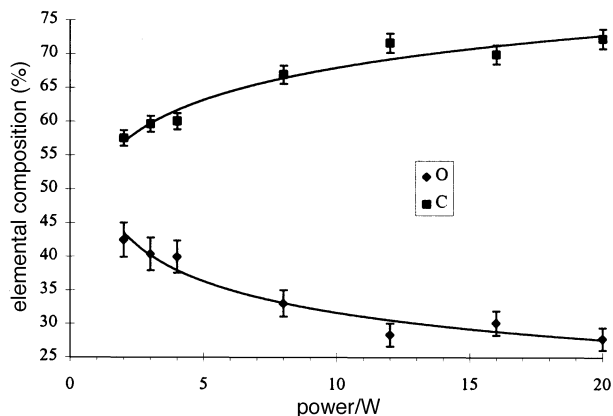


Fig. 2 Deposition rate of ppAAc as a function of plasma power for a constant acrylic acid flow rate (5 sccm)



**Fig. 3** The effect of plasma deposition power upon the elemental composition determined by XPS of plasma polymerised acrylic acid at a monomer flow rate of 5 sccm

reported in a forthcoming publication on the physicochemical properties of ppAAc.

### XPS

**Elemental composition.** The XPS analysis of ppAAc deposited over a range of powers detected the presence of only carbon and oxygen. This indicated that the aluminium substrate was covered with a thickness greater than the analysis depth of XPS ( $\approx 8$  nm for Al 2p photoelectrons) and that no significant back streaming of the pump oil (fluorine containing) occurred. Quantification of spectra acquired from films deposited over a range of  $P$  at a constant flow rate provided the elemental compositions presented in Fig. 3. These data illustrate that increasing  $P$  reduces the oxygen concentration of the deposit from  $42 \pm 4.2$  to  $28 \pm 2.8\%$ , *i.e.* from the elemental composition of acrylic acid/PAA to a deposit with a deficiency of oxygen.

**Functional composition.** The XPS C 1s peaks from films formed at the extremes of deposition power considered in this work ( $P=2$  and 20 W) are presented in Fig. 4. The high binding energy peak [C(=O)OX], and the associated  $\beta$ -shifted carbon [C-C(=O)OX] indicate the presence of carboxy groups (where X=H) and/or ester (where X=R) and/or anhydride (where X=O-C(=O)) functionality. It is apparent from the C 1s peak shape (Fig. 4, inset) that deposition at high plasma power ( $P=20$  W) produced a deposit with a low relative intensity of this component compared to a deposit produced at a low power ( $P=2$  W). The C 1s peaks from deposits formed across the power range were curve fitted using a standard procedure. These data, presented in Fig. 5, indicate a gradual transition of the form of the C 1s peak between films deposited at  $P=2$  and 20 W.

**Derivatisation.** To enable the unambiguous identification, and quantification, of the C(=O)OX carbon functionalities it is necessary to use TFE derivatisation. In the vapour phase the TFE molecule reacts with carboxylic acid but not esters or hydroxy functionalities.<sup>16</sup> Reaction of TFE has been reported with epoxides and may occur with anhydrides. We assume that in our samples epoxides are not present in significant quantities and, should anhydrides be formed in the deposits, they would be hydrolysed in the atmosphere to form acids. Therefore, the level of fixation as determined by XPS may be used to calculate the relative proportion of acid and ester present in the plasma polymer.

It was necessary to construct a TFE fixation *versus* time curve in order that full derivatisation could be confirmed for ppAAc produced at both extremes of  $P$ . The fixation of TFE was followed through the F/C ratio plotted in Fig. 6. The form

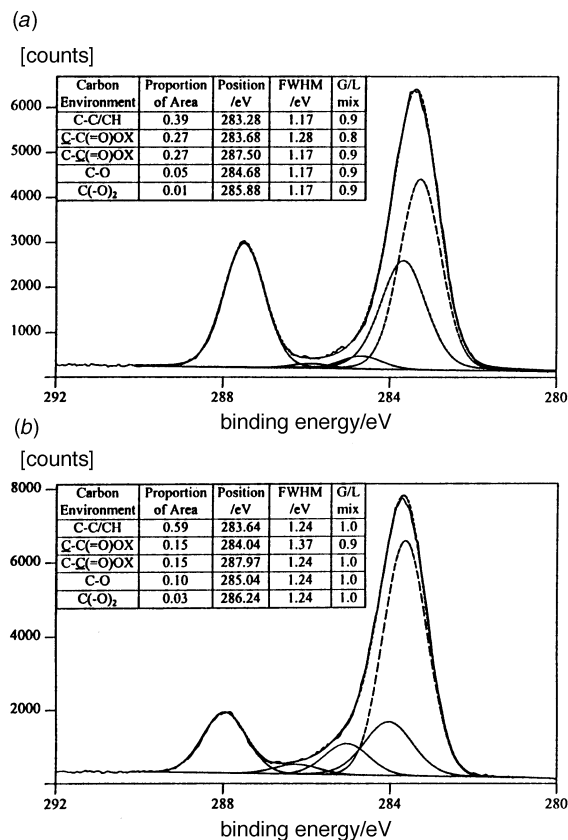


**Fig. 4** XPS C 1s peak from ppAAc produced at (a)  $P=2$  W and (b)  $P=20$  W

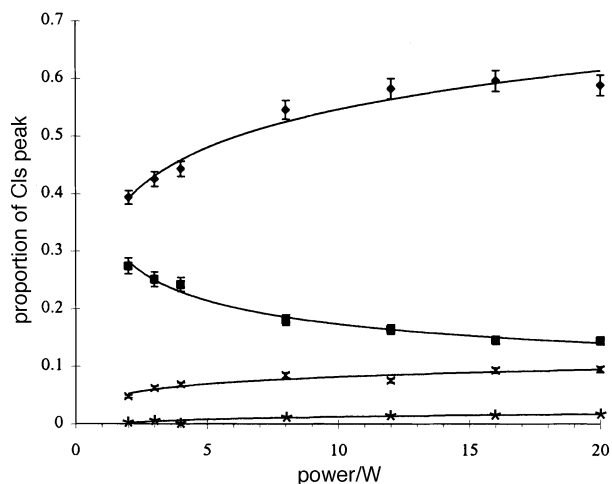


**Fig. 5** The effect of plasma deposition power upon the functional composition of acrylic acid deposits as determined from the XPS C 1s peak: (◆) C-C, (■) C(=O)-O, (×) C-O and (\*)C(-O)<sub>2</sub>

of the curves for ppAAc deposited at both  $P=2$  and 20 W indicated that no significant TFE uptake occurred after 3–5 h of exposure. This time to saturation is compatible with stoichiometric reaction of the TFE molecule with carboxy functionalities.<sup>17</sup>

Curve fitting of the C 1s peaks acquired from TFE labelled ppAAc,  $P=2$  and 20 W, is presented in Fig. 7. The proportion of carbon present as carboxylic acid functionalities at the surface of the plasma polymers is presented in Table 1. Using the  $CF_3/C(=O)OX$  ratio (from the TFE labelled sample) a measure of the proportion of C(=O)OX carbon environments which were carboxy groups was obtained. Using this method it was calculated that 82% of the C(=O)OX functionalities in 2 W deposit were carboxy groups, while for the  $P=20$  W

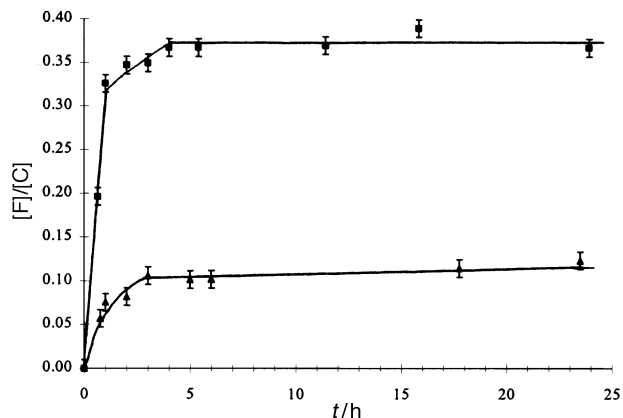


Fig. 6 TFE reaction versus exposure time for ppAAc deposited at (■) 2 W and (▲) 20 W

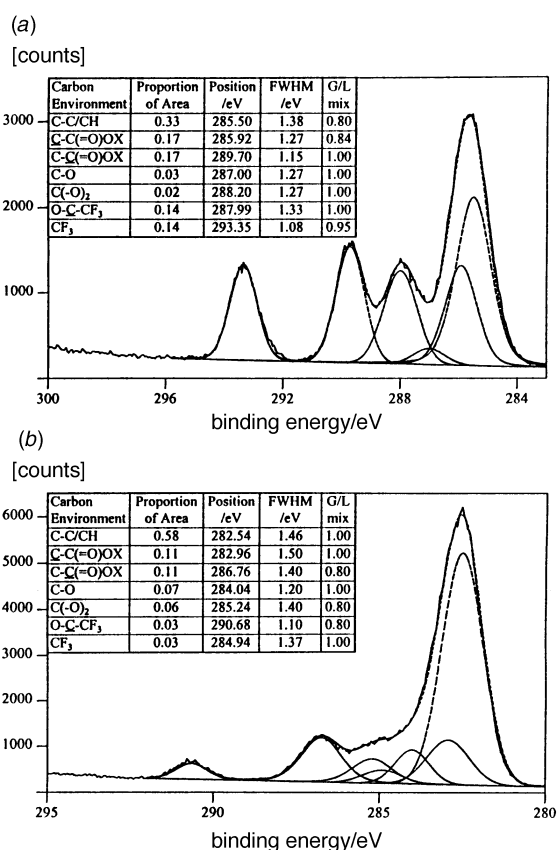


Fig. 7 XPS C 1s peaks from plasma polymerised acrylic acid deposited at (a)  $P=2$  and (b)  $P=20$  W followed by TFE derivatisation

material the proportion was only 27%. These results correspond to a retention of acid functionalities (relative to the monomer) of 0.22/0.33 = 66% and 0.04/0.33 = 12%, for  $P=2$  and 20 W respectively.

If we assume that the ppAAc includes only carboxylic acid, ester, ketone/aldehyde, alcohol and ether functionalities we can calculate the functional composition of the deposits using these results. In addition, it is implicit in the curve fitting methodology that the  $\beta$ -carbon atoms assigned to the carboxy group functionalities were not directly combined with oxygen atoms. Thus, in Table 1 we are able to assign all of the functional groups for both extreme deposition conditions ( $P=2$  and 20 W). The full assignment of the carbon functionalities gives us confidence in these assumptions.

**Valence bands.** The valence band spectra (0–35 eV) were acquired from  $P=2$  and 20 W ppAAc deposits (Fig. 8). These

Table 1 Plasma polymer functional composition as a proportion of carbon calculated from the XPS analyses of TFE ppAAc, where X represents CH<sub>3</sub>, H or CH<sub>2</sub>

		composition of ppAAc (%)	
		2 W	20 W
elemental composition	[C]/[O]	58/42	72/28
proportion of C present as carboxylic acid	C(=O)OH	22	4
thus, proportion of C present as ester	C(=O)O-C	5	11
proportion of C present as ester functionalities	C(=O)O-C	5	11
proportion of C in hydroxy functionalities	C-OH	0	0
proportion of C involved in ether functionalities	C-O-C	0	0
proportion of C involved in carbonyl functionalities	C=O	1	3
proportion of C involved in non-functional carbon [CH <sub>2</sub> /C-C] from C 1s	CH <sub>2</sub> /C-C	66	74

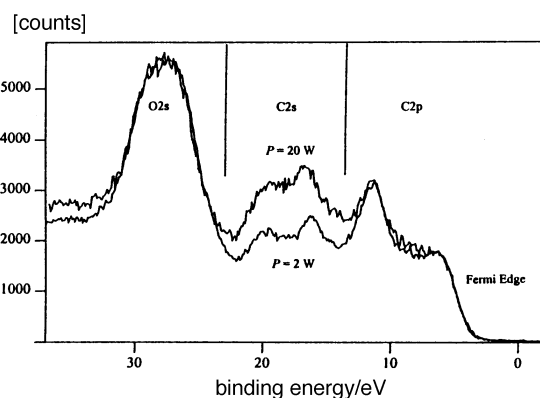


Fig. 8 Valence band spectra from ppAAc deposited at  $P=2$  and 20 W

were shifted and scaled for comparison using the position of the C 1s peak (285.0 eV) and the intensity of the Fermi Edge (2–6 eV) respectively. It is apparent that while the O 2s (25–30 eV) and C 2p (5–12 eV) regions changed little between the two deposits, the C 2s region (13–21 eV) was significantly different. This region has previously been assigned to C–C  $\sigma$ -bonds.<sup>18</sup> Therefore, the increased relative intensity within this region for the  $P=20$  W deposit is attributed to an increase in C–C bonding in this sample. Comparison of these spectra with those included in a polymer database including valence band spectra<sup>15</sup> reveals that the form of the spectra for the 2 W is very similar to that for PAA. An increase in the intensity of the C 2s region is seen in the spectra of poly(methacrylic acid) where a backbone H is substituted by a methyl group substantiating the conclusion that the higher plasma power ( $P=20$  W) increases the degree of C–C bonding in the deposit. The poorly defined nature of this change in the spectra from the plasma polymers, relative to the polymer standards, is indicative of the diversity of hydrocarbon states. This is consistent with the changes in the atomic ratio (Fig. 3) and functional composition (Fig. 5).

## SIMS

**Poly(acrylic acid) (PAA).** Positive and negative ion SIMS spectra of PAA<sup>19</sup> were studied to determine the peaks seen in SIMS for a fully linear conventional polymer of acrylic acid. The negative ion spectrum from PAA was found to provide the most useful structural information. Peaks diagnostic of the polymer structure were observed at multiples of the monomer

repeat unit at  $m/z$  71, 143, 215 and 287, assigned to the structures:  $\text{H}[\text{CH}_2-\text{CH}(\text{COOH})]_n-\text{CH}=\text{CH}-\text{C}(=\text{O})\text{O}^-$ , where  $n=0-3$ .

Assignment of cyclic structures are also possible for the ions at  $m/z$  215 and 287.

These ions are characteristic of methyl-terminated end-groups in the polymer. The dominance of the SIMS spectra by end-groups has recently been determined in low molecular weight PMMA.<sup>20</sup> The fragments are produced in the SIMS process by the scission of one backbone bond which produces the carbon double bond. Loss of a proton results in the formation of the carboxylic anion. Fragments of the  $m/z$  71 ion were observed at  $m/z$  41 and  $m/z$  59 corresponding to the structures,  $\text{HC}\equiv\text{C}-\text{O}^-$  and  $\text{CH}_3-\text{C}(=\text{O})-\text{O}^-$  respectively. At higher mass, ions terminated by structures of the former type were observed at  $m/z$  113, 185 and 257, equivalent to the loss of  $\text{H}_2\text{C}=\text{O}$  from the species illustrated above.

**ppAAc  $P=2$  W.** The negative ion SIMS spectra from a 2 W ppAAc deposit is presented in Fig. 9(a). It is apparent that the spectrum from the plasma polymer contains all the peaks of conventional PAA, from  $n=0-3$ , although the relative peak intensities differ. These ions emanate from structures at the surface of the plasma polymer which are equivalent to the end-groups observed in the PAA spectra discussed above and shall be referred to as type I ions. Furthermore, where in the conventional polymer a single peak was present at  $m/z$  71 (143, 215 and 287), in the plasma polymer an additional peak was seen at  $m/z$  73 (145, 217, 289 and 361). These were assigned with ions of the structure:  $\text{H}-[\text{CH}_2-(\text{COOH})\text{CH}]_m-\text{CH}_2-\text{CH}_2-\text{C}(=\text{O})\text{O}^-$ , where  $m=0-4$ .

This type of ion contains two saturated end-groups suggesting that it emanates from physisorbed oligomer and/or through

the scission of ester linkages. It is not possible to differentiate these two possible surface structures from the SIMS data. These ions shall be referred to as the type II ions.

**ppAAc  $P=20$  W.** In contrast to the SIMS spectrum from the  $P=2$  W deposit the spectrum from the  $P=20$  W deposit had no contribution from ions containing more than two acrylic acid repeat units ( $m/z$  145) [Fig. 9(b)]. Furthermore, the intensity of the type II ion ( $m/z$  73) was observed to be greater than that of the type I ion ( $m/z$  71). The higher ester content of this sample has already been determined in the XPS section above. This correlation of type II ions with esters leads us to assign them to ester bound structures and not physisorbed species.

Reevaluating the data in Fig. 9(a) ( $P=2$  W) with this information, we may conclude that we have carbon-bound structures (type I ions) up to  $n=3$  and ester-bound structures (type II ions) up to  $m=4$ . It is notable that the type II ion at  $m/z=217$  ( $m=2$ ) is of a relatively low intensity. We attribute this to the enhanced stability of the cyclic type II ion ( $n=4$ ) at  $m/z=215$ .

The spectral intensity detected from the  $P=20$  W sample (0.06 ions per pulse) was substantially lower than that observed from the  $P=2$  W deposit (0.19 ions per pulse). Additionally, the hydrogen peak [off-scale in Fig. 9(b)], exhibits a higher relative intensity in the spectrum of the  $P=20$  W film. The dependence of overall ion yield on the degree of end-groups relative to backbone structures,<sup>20</sup> and the increased contribution of atomic ions to spectra from cross-linked plasma polymers<sup>21</sup> have both previously been reported. Thus the absolute and relative ion intensities in the spectrum from the  $P=20$  W when compared with that of the low power deposit suggest the presence of cross-linked material.

## Discussion

### Deposit structure

Deposition rate data (Fig. 2) is consistent with the two deposition regimes termed by Yasuda the *energy-deficient regime* at low power and the *monomer-deficient regime* at high power.<sup>1</sup> In our system  $P=4$  W defines the boundary between these two regimes. The quantitative analysis of films obtained by XPS illustrates that the elemental (Fig. 3) and functional composition (Fig. 5) of ppAAc changes progressively between these two deposition regimes.

The combination of TFE derivatisation and XPS provides an unambiguous quantitative description of the plasma polymer functionality at the two extremes of power ( $P=2$  and 20 W) (Table 1). Films made at low power ( $P=2$  W) have an elemental and functional composition which is close to that of the acrylic acid/PAA, *i.e.* with 66% of the carbon present as hydrocarbon (equal to the monomer), 22% acid (66% of the monomer) and the remaining present as ester (10%) and ketone/aldehyde (1%). Thus, in the deposition process the carboxy groups that are not present in the deposit (relative to the monomer) have been converted into esters, and to a very limited extent ketone/aldehydes. SIMS data from  $P=2$  W deposit indicates the presence of linear structures containing up to five acrylic acid units, as found in the spectrum from PAA. In addition, the spectrum of ppAAc reveals additional ions (type II) which are assigned to ions produced from the scission of an ester linkage in the SIMS process. Thus at low plasma powers where there is a 'deficiency' of power the resultant deposit is very similar to conventional PAA with the exception that 10% of the carboxy carbons have been converted into ester functionalities.

At high plasma power ( $P=20$  W), the proportion of hydrocarbon and ester in the films increases to 74 and 22% respectively, while the acid falls to 4% (12% that of the

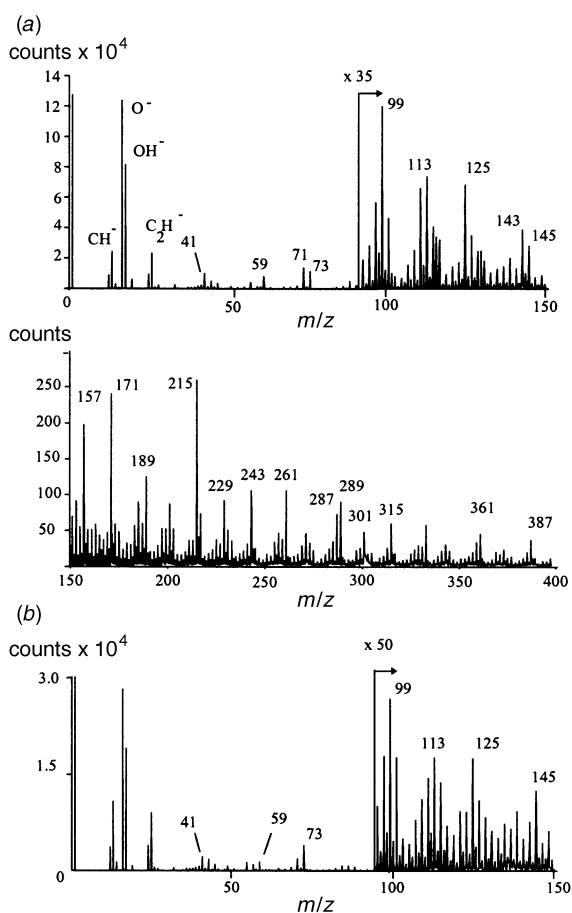


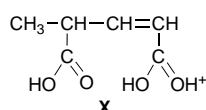
**Fig. 9** Negative static SIMS spectra of ppAAc at (a)  $P=2$  and (b)  $P=20$  W (the hydrogen peak,  $5 \times 10^4$  counts, is off-scale)

monomer). Thus, in the monomer deficient regime the conversion of the acrylic acid carboxy group into esters is clearly favoured. SIMS identifies a decrease in the abundance and size of linear structures in the deposit such that the dimer of the acrylic acid molecule is the largest ion observed (at low intensity), *i.e.* the deposit is very unlike PAA. Instead the SIMS, XPS and valence band data indicate a deposit cross-linked through C—C bonds in which the majority of acid functionalities have been converted into esters. Increased cross-linking in plasma polymers is often observed at high deposition power.<sup>1,2</sup> This effect of plasma power is rationalised as an increase in the range of available reaction pathways as a result of greater monomer fragmentation. In the plasma polymerisation of acrylic acid it is clear that the increase in plasma power facilitates significant ester formation.

### Mechanism of deposit formation

O'Toole *et al.* have carried out mass spectrometry on acrylic acid plasmas.<sup>10</sup> This data on the plasma species allowed them to postulate deposition mechanisms which we discuss below in the light of our data on the chemistry of ppAAc.

**Power deficient regime.** As discussed above, the chemistry of films formed at low plasma powers ( $P=2$  W) closely resembles the chemistry of PAA. O'Toole *et al.* detected oligomers up to three monomer units in the positive mass spectrum of low power acrylic acid plasmas which they proposed were formed through positive ion—molecule reactions, *e.g.* structure X.



Comparison with XPS analysis of films deposited from these plasmas led the authors to argue that such ions were responsible for the carboxylic acid functionalisation of the polymer product. Our SIMS data provides direct evidence for the existence of related species in the  $P=2$  W deposit, *i.e.* type I and II ions detailed in the section SIMS above. To explain the structures determined to exist in the deposits by SIMS it is necessary that these cations combine with surface species to form both C—C bonds and ester linkages. The latter case is discussed in the next section with reference to the monomer-deficient regime where it is dominant. The former case may take place in a manner analogous to that proposed in the plasma phase by O'Toole *et al.*, *i.e.* in place of reaction with the monomer molecules in the gas phase the positively charged oligomers react with surface species. For the formation of a C—C bond (to result in type I SIMS structures), this necessitates an internal rearrangement (of structure X) such that proton transfer occurs from the carbonyl oxygen to the alkene and the secondary carbocation so generated reacts with the deposit.

The disparity between the maximum number of monomer repeat units detected in the plasma (3) and in the deposit (5) may result from either the very different detection conditions of the two analysis techniques (quadrupole plasma mass spectrometry and reflection TOF SIMS), or the different deposition configurations. Comparison of our data with the C 1s data of O'Toole *et al.* suggests that the latter explanation may be at least partly responsible as their highest retention deposit appears to have a lower retention than the deposits from which our SIMS data was obtained. Our identification of a significant proportion of esters in ppAAc deposits suggests their retention of 71%, calculated from the C(=O)X component of the C 1s peak, to be an overestimate.

This correlation of deposit molecular structure (SIMS) and plasma-phase oligomers (plasma-phase MS) is part of a significant amount of evidence from a number of plasma polymer

systems indicating that the role of the positive ions in deposit formation at low plasma power is underestimated<sup>21,22</sup> This data contrasts with the traditional view that deposit formation proceeds through the combination of neutral species.

**Monomer deficient regime.** At high plasma power ( $P=20$  W) the oxygen content of the film has fallen from  $42 \pm 4.2\%$  ( $P=2$  W) to  $28 \pm 2.8\%$ . This indicates a preferential loss of oxygen in the form of gaseous products and/or preferential incorporation of carbon into the deposit. The fragmentation of acrylic acid under electron impact to form CO and CO<sub>2</sub> has previously been noted, as has the tendency to lose H<sub>2</sub>O in the plasma environment.<sup>8,10</sup> Therefore, we propose that this decrease in the carbon content of the film is related to the increased fragmentation of the monomer to form these species which are not readily incorporated in the deposit. Valence band data indicates increased C—C  $\sigma$ -bonding in the high power deposits. This is consistent with an increase in cross-linking in this deposit also noted in the SIMS spectra. Thus the greater fragmentation of the monomer in the monomer-deficient regime results in an increase in the reaction pathways available which manifests itself as a deposit containing more cross-linking and esters.

The presence of esters in ppAAc has not previously been unambiguously identified because derivatisation of the carboxy groups was not undertaken.<sup>4,5,7,10</sup> In the most thorough mechanistic study of polymerisation in acrylic acid plasmas to date no mechanism for the formation of esters was proposed because no evidence for esters in the plasma was obtained.<sup>10</sup> Therefore, we conclude that ester linkages form at the surface of the deposit through interaction of the neutral or positive plasma species.

### Interaction of ppAAc with acrylic acid and water vapour

It is interesting to note that no permanent weight increase was observed upon exposure of the freshly prepared film to the atmosphere. It is often reported in the literature that the flow of the monomer is maintained for some time after the plasma is turned off, before venting of the chamber to the atmosphere, to encourage reactive surface species to react with monomer, *e.g.* free radicals. Our data indicate that a significant concentration of reactive species does not exist at the surface when the plasma is extinguished because no permanent weight increase occurred. The deposits did not pick up nitrogen or oxygen upon storage and indicated no reactivity with the atmosphere after production of the type often observed for plasma treated polymers.<sup>23</sup> This indicates that significant plasma etching or UV bombardment of the deposits did not occur. The presence of absorbed water in ppAAc will have significant implications for the application of ppAAc and will most probably be a contributing factor to the ageing phenomena previously identified in similar deposits when stored under humid conditions.<sup>5</sup> This may have implications in the proposed application of ppAAc in adhesion promotion as the presence of water at the interphase is usually associated with poor joint durability.<sup>24</sup>

### Conclusions

Acrylic acid has been plasma polymerised to form deposits with between 66 and 12% retention of the carboxy group by varying the plasma power between  $P=2$  and 20 W respectively. Low plasma power deposits ( $P=2$  W) exhibited high functional retention and a chemistry similar to that of PAA. Deposit formation at higher powers ( $P=20$  W) was characterised by the preferential formation of esters and cross-linking.

In high retention deposit ( $P=2$  W) linear species containing up to five acrylic acid repeat units have been detected by SIMS. At high plasma power ( $P=20$  W) no linearity greater

than two acrylic acid units was observed. This detection of these molecules reinforces the argument, based on plasma-phase mass spectrometry observations,<sup>10</sup> that positively charged oligomeric plasma species are responsible for functional retention in ppAAc. Furthermore, the absence of structures containing ester functionality in the published plasma-phase mass spectrometry data suggest that ester formation occurs at the deposit surface.

Deposit weight changes showed that in atmosphere ppAAc films absorb a significant amount of water.

Funding for the development of the plasma reactor came from Daimler Benz, whilst the Marie Curie fellowship for Morgan Alexander was provided by the European Commission (Contract No: ERBFMBICT960801). Support for this work from Franz Gammel and H. Suchentrunk of Daimler Benz (Ottobrunn, Germany) and Eoghan McAlpine of Alcan International (Banbury, UK) is gratefully acknowledged. Assistance from Marc Botreau and Didier Parrat in the acquisition of the SIMS and XPS data respectively is acknowledged. John Treverton and Georg Wachinger (Daimler) are thanked for their initial interest in this topic.

## References

- 1 *Plasma Polymerisation*, ed. H. K. Yasuda, Academic Press, London, 1985.
- 2 *Plasma Deposition, Treatment and Etching of Polymers*, ed. R. d'Agostino, Academic Press, London, 1990.
- 3 E. S. Lopata and J. S. Nakanishi of *The BOC Group Inc. Process for plasma enhanced chemical vapour deposition of anti-fog and anti-scratch coatings onto various substrates U.S. Pat. No 5 487 920*, 30th Jan. 1996.
- 4 Y. Novis, M. Chtaïb, R. Caudano, P. Lutgen and G. Feyder, *Brit. Polym. J.*, 1989, **21**, 171.
- 5 D. L. Cho, P. M. Claesson, C-G. Gölander and K. Johansson, *J. Appl. Polym. Sci.*, 1990, **41**, 1373.
- 6 T. J. Lin, B. H. Chun, H. K. Yasuda, D. J. Yang and J. A. Antonelli, *J. Adhesion Sci. Technol.*, 1991, **5**, 893.
- 7 T.-M. Ko and S. L. Cooper, *J. Appl. Polym. Sci.*, 1993, **47**, 1601.
- 8 A. P. Ameen R. D. Short and R. J. Ward, *Polymer*, 1994, **35**, 4382.
- 9 A. J. Ward and R. D. Short, *Surf. Interfac. Anal.*, 1994, **22**, 477.
- 10 L O'Toole, A. J. Beck, A. P. Ameen, F. R. Jones and R. D. Short, *J. Chem. Soc., Faraday Trans.*, 1995, **91**, 3907.
- 11 A. J. Beck, F. R. Jones and R. D. Short, *Polymer*, 1996, **37**, 5537.
- 12 A. P. Kettle, A. J. Beck, L. O'Toole, F. R. Jones and R. D. Short, *Composites Science and Technology*, 1997, **57**, 1023.
- 13 A. P. Kettle, F. R. Jones, M. R. Alexander, R. D. Short, W. Wu, I Verpoest and M. Stollenwerk, *Composites Part A*, 1997, **29**, 241.
- 14 S. Tanuma, C. J. Powell and D. R. Penn, *Surf. Interfac. Anal.*, 1991, **17**, 911.
- 15 Beamson and Briggs, *High Resolution XPS of Organic Polymers—The Scienta ESCA300 Database*, Wiley, Chichester, 1992.
- 16 Chilkoti, B. D. Ratner and D. Briggs, *Chem. Mater.*, 1991, **3**, 51.
- 17 M. R. Alexander, P. V. Wright and B. D. Ratner, *Surf. Interfac. Anal.*, 1996, **24**, 217.
- 18 D. G. Castner and B. D. Ratner, *Surf. Interfac. Anal.*, 1990, **15**, 479.
- 19 Spectrum of poly(acrylic acid) in preparation for submission to The Static SIMS Library, Surface Spectra Ltd., Manchester, 1998 ed. J. C. Vickerman, D. Briggs and A. Henderson.
- 20 A. M. Leeson, M. R. Alexander, R. D. Short, D. Briggs and M. J. Hearn, *Surf. Interfac. Anal.*, 1997, **25**, 361.
- 21 M. R. Alexander, R. D. Short and F. R. Jones, *RF HMDSO plasma deposition: A comparison of plasma- and deposit-chemistry, Plasmas and Polymers*, in press, 1997.
- 22 L. O'Toole and R. D. Short, *J. Chem. Soc., Faraday Trans.*, 1997, **93**, 1174, and the references cited therein.
- 23 R. F. France and R. D. Short, *Polym. Degrad. Stability*, 1994, **45**, 339.
- 24 J. F. Watts *Surf. Interfac. Anal.* 1988, **12**, 497.

Paper 7/08064F; Received 10th November, 1997